

Chemical, thermophysical, rheological, and microscopic characterisation of rubber modified asphalt binder exposed to UV radiation

Mehdi Zadshir, Desiree Ploger, Xiaokong Yu, Cesare Sangiorgi & Huiming Yin

To cite this article: Mehdi Zadshir, Desiree Ploger, Xiaokong Yu, Cesare Sangiorgi & Huiming Yin (2020): Chemical, thermophysical, rheological, and microscopic characterisation of rubber modified asphalt binder exposed to UV radiation, Road Materials and Pavement Design, DOI: [10.1080/14680629.2020.1736606](https://doi.org/10.1080/14680629.2020.1736606)

To link to this article: <https://doi.org/10.1080/14680629.2020.1736606>



Published online: 11 Mar 2020.



Submit your article to this journal [↗](#)



View related articles [↗](#)



View Crossmark data [↗](#)



Chemical, thermophysical, rheological, and microscopic characterisation of rubber modified asphalt binder exposed to UV radiation

Mehdi Zadshir^a, Desiree Ploger^b, Xiaokong Yu^a, Cesare Sangiorgi^b and Huiming Yin^{a*}

^aDepartment of Civil Engineering and Engineering Mechanics, Columbia University, New York, NY, USA; ^bDepartment of Civil, Chemical, Environmental, and Materials Engineering, University of Bologna, Bologna, Italy

(Received 31 January 2019; accepted 18 February 2020)

In this work, the effect of ultraviolet (UV) radiation on samples of asphalt binder mixed with crumb rubber is studied. Two sets of samples are characterised using a PG 64-22 neat binder with different percentages of rubber particles being 0, 16.6, and 20.0 wt.%. One set of the samples was stored at ambient temperature (called the unaged set) and the other was inserted inside an accelerated weathering tester for 100 h (called the UV-aged set). Thermal conductivity, chemical indices, rheology, and morphology of both sets of samples are tested using the flash method, differential scanning calorimeter (DSC), Fourier-Transform Infrared Spectroscopy (FTIR), dynamic shear rheometer (DSR), and Scanning Electron Microscope (SEM), respectively. Results show that the addition of rubber leads to a reduction of specific heat for the rubber-modified binders. Specific heat capacities of the three UV aged samples are larger than those of their unaged counterparts, and the 16.6%-aged has the highest value. FTIR spectra of the three unaged samples are very similar, whereas distinct changes occur after UV exposure. The normalised absorbance of the peak associated with S = O group increases and the peak for the aliphatic group decreases after UV aging, showing some evidence of oxidation due to UV aging. Use of crumb rubber in the binder decreases the thermal conductivity and 20.0 wt.% sample is even less conductive compared to the 16.6 wt.%. At all temperatures above 25°C, aged samples have lower thermal conductivity than the unaged ones, except neat binder which is opposite. Rheological measurements show that the complex modulus of the samples increases with the addition of rubber particles and also after aging. However, 16.6% rubber-modified sample shows the least increase in modulus after aging. Microscopic morphology shows that UV radiation causes cracks in both neat and rubber modified binder. Smaller cracks are seen to form, and the cracked pieces are stuck together in the rubber modified binders, whereas less cohesion between the cracks is observed in the neat binder.

Keywords: Crumb rubber; UV aging; asphalt binder; thermal conductivity; rheology; chemical characterisation; surface cracks

Background

Many researchers in recent years have studied the aging mechanism of asphalt binders by doing laboratory experiments or computer simulations. Asphalt aging is explained by two main mechanisms: the oxidation of functional groups in asphalt and the volatilisation of its light molecular components, which function as peptising agents (Lu & Isacson, 2002; Qin et al., 2014a; Yu et al., 2014). Through these two aging mechanisms, the concentration of asphaltenes and resins

*Corresponding author. Email: yin@civil.columbia.edu

in asphalt binder often increases, making the binder stiffer and more brittle (Lu & Isacsson, 2002). The aging mechanism for rubber modified binder is even more complex than the neat binder, because of the dynamic nature of crumb rubber (CR) particles in the asphalt, and the effects of time and temperature on the enhancement of the physical properties of the rubber-modified binder (Bahia et al., 1998). CR particles absorb aromatics in asphalt and swell three to five times their original size at elevated temperatures (Lo Presti, 2013; Medina & Underwood, 2017). However, they do not reach their maximum level of swelling during the interaction period (Abdelrahman & Carpenter, 1999), which leads to the different behaviour of asphalt binder during the aging processes with oxidation, volatilisation, and degradation (Huang & Pauli, 2008). It is known that polymeric components can affect the aging mechanism of asphalt (Lu & Isacsson, 2002; Ruan et al., 2003; Wu et al., 2012; Yildirim, 2007). Polymeric chains function as retardants in asphalt and hinder the penetration of oxygen molecules while reducing the oxidation rate of asphalt's functional groups (Lewandowski, 1994; Lu & Isacsson, 1998). Polymeric chains may degrade during aging and consequently neutralise part of the physical hardening that occurs as a result of the oxidation and volatilisation of asphalt components (Cortizo et al., 2004; Ouyang et al., 2006).

Among all the environmental factors that affect the long-term performance of the pavement, the photo-oxidation of the binder by the ultraviolet (UV) spectrum of sunlight is a phenomenon that has gained more attention recently (Yi-Qiu et al., 2008; Zadshir et al., 2018). In general, the physicochemical interactions between the asphalt and the crumb rubber (CR) particles that occur when subjected to UV aging alter the thermophysical properties of the CR-modified binder and accordingly, influencing the pavement's performance. One of the most important thermophysical parameters of asphalt is its thermal conductivity that affects the heat transfer in asphalt pavements. Specifically, the thermal conductivity of asphalt binders contributes to the temperature distribution in asphalt pavements and thus, affects the viscoelastic modulus and the temperature profile near the pavement surface (Mrawira & Luca, 2002).

In a substance with high thermal diffusivity, heat moves rapidly through the substance, and it generally does not require much energy from its surroundings to reach thermal equilibrium and vice versa (Pietrak & Wiśniewski, 2014). CR-modified binders deserve particular attention since their thermal conductivities and diffusivities are affected by the ratio change (Chen et al., 2015). Rubber is usually applied as a thermal insulation material in buildings for its low thermal conductivity and therefore, adding CR to the asphalt binder may influence the thermal conductivity and the temperature distribution within the asphalt pavement, which consequently affects the rutting resistance of pavement (Tarefder et al., 2003).

The objective of this study is to investigate the influence of UV exposure on the chemical, thermal, rheological, and microscopic structure of a neat binder as well as modified ones with different contents of Crumb Rubber (CR) at their service temperatures. In the following, asphalt binders with different contents of crumb rubber powder (0%–neat binder, 16.6%, 20.0%) are prepared and then exposed to the ultraviolet rays. The aging effects due to the UV exposure and the role of crumb rubber modifier are evaluated with various chemical characterisation tests and optical methods being FTIR, DSC, Nanoflash, DSR, and SEM.

Materials and methods

Preparation of the samples

Neat binder (PG 64-22) was obtained from Peckham Industries, Inc. (Bronx, New York, USA). Characteristics of the neat binder as obtained from the supplier are shown in Table 1. Crumb rubber (CR) particles with an average size of 0.42 mm and a relative density of 0.46–0.51 g/cm³

Table 1. Penetration, viscosity, and specific gravity of the neat binder PG 64-22.

| Property | Value |
|-------------------------------|-------|
| Penetration at 25°C (1/10 mm) | 65 |
| Viscosity at 135°C (cSt) | 493 |
| Viscosity at 165°C (cSt) | 135 |
| Specific gravity at 15°C | 1.043 |
| Specific gravity at 25°C | 1.037 |

were obtained from Albatros Ecologia Ambiente Sicurezza Soc. Cons. a r.l. (Italy). The rubber powder consists of vulcanised rubber polymer, carbon black, zinc oxide, magnesium silicate, aluminium silicate, and extender oil.

To make CR-modified binder, ASTM D6114M-09 standard suggests that rubber-modified binder should have at least 15 wt.% of rubber, and standards from other states or countries defined a rubber content of 15–24 wt.% (Lo Presti, 2013). The weight ratio in these standards is defined as:

$$\%wt. = \frac{\text{Weight of crumb rubber}}{\text{Weight of crumb rubber} + \text{weight of neat binder}} \quad (1)$$

In this paper, the authors chose to make two different weight ratios of CR-modified binders, 16.6 and 20.0 wt.% following the above formula. The two rubber-modified binders were made using the “wet-process”: (1) a clean glass beaker was weighted and zeroed on a scale; (2) hot neat binder (preheated to $\sim 130^{\circ}\text{C}$) was poured into the beaker, and the net weight of the neat binder was recorded (with a precision of ± 0.01 g) and then the beaker with the neat binder was placed onto a hot plate (temperature set at 190°C); (3) the right amount of crumb rubber according to the designed ratio was weighted; (4) a shear mixer, centred on top of the beaker, was used to stir the hot neat binder, while slowly the crumb rubber particles were added into the hot liquid bitumen. The shear speed of the mixer was set at 600 rpm, and the mixing process lasted for almost 60 mins. The height of the mixer blades was adjusted at 20 and 40 mins after the beginning of the mixing process to achieve a more uniform mix as the volume of the binder increased.

To prepare the samples to be exposed to UV rays, the ASTM D1669 Standard “Practice for Preparation of Test Panels for Accelerated and Outdoor Weathering of Bituminous Coatings” was used with some modifications (Zadshir et al., 2018). For this paper, three types of samples were prepared; one for running Fourier-transform infrared spectroscopy (FTIR) test, and the other two of similar designs yet with different thicknesses for running dynamic shear rheometer (DSR) and Nanoflash, as shown in Figure 1. The neat and the rubber-modified samples were then poured onto the aluminium plates that were covered with UV resistant tape and heat pressed to reach the desired thickness. One set of all the samples was kept at room temperature as the reference (Unaged samples) whereas, the other set was inserted inside a weathering chamber so that the specimens could be exposed to the UV rays (Aged samples).

UV aging: QUV accelerated weathering tester

The samples are conditioned in a QUV Accelerated Weathering Tester, which resembles the damage caused by weather and ultraviolet (UV) rays of sunlight (Figure 2(a)). In this instrument, fluorescent UV lamps simulate the wavelength of sunlight. The QUV can accelerate effects due to UV rays and weathering conditions in a few days that will actually happen in months or years of outdoor exposure. It uses alternating cycles of UV, moisture (if selected), and condensation

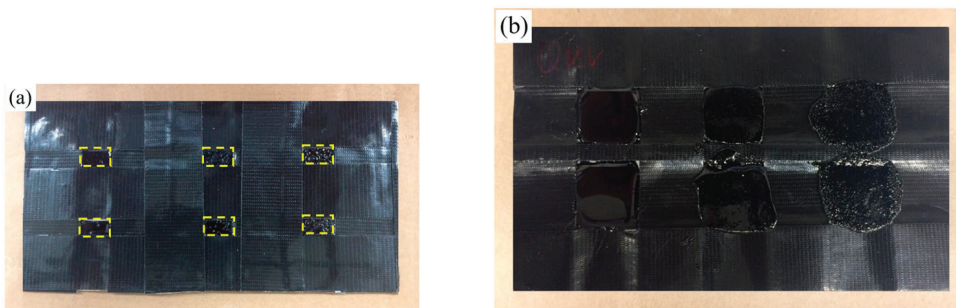


Figure 1. (a) Prepared samples for FTIR with a dimension of 1.27 cm \times 0.63 cm (0.5 in \times 0.25 in), (b) prepared samples for DSR and Nanoflash, with a dimension of 3.17 cm \times 3.17 cm (1.25 in \times 1.25 in).

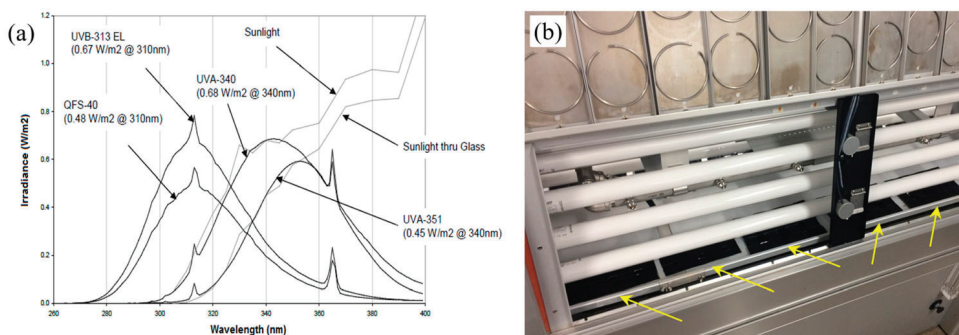


Figure 2. (a) Comparison of UV lamps wavelength with sunlight, (b) neat and rubber-modified asphalt samples in the QUV tester.

at controlled elevated temperatures to expose the samples to weathering conditions. The UVA-340 lamp with a peak emission of 340 nm provides the best simulation of the sunlight in the critical short wavelength region from 365 nm down to the solar cutoff of 295 nm (Figure 2(a)). In this study, the ASTM 4799 standard practice for “Accelerated Weathering Test Conditions and Procedures for Bituminous Materials” was used as a reference. The samples were placed at the bottom of the instrument (Figure 2(b)) and were exposed to 100 h of UV aging with a radiation intensity of 0.89 W/m².nm and a reduced temperature of 45°C (i.e. the lowest operating temperature that this instrument allows). This temperature setting is based on the findings from Zeng et al. (2015) that the influence of temperature can be neglected if it is below 50°C. Each cycle included 8 h of UV light followed by 4 h of rest period, simulating the nighttime. After the conditioning was finished, the samples were removed from the QUV instrument and used for running the FTIR, DSC, Nanoflash, and DSR tests.

Fourier-transform infrared spectroscopy (FTIR)

The Thermo Scientific Nicolet iS50 FT-IR Spectrometer was used to acquire the spectra of each sample to study changes in their chemical functional groups due to the addition of rubber particles and the UV aging. For unaged samples, a small number of materials was taken from random locations of the container in which the samples were stored. For UV aged samples, a thin layer (less than 1 mm) of material was taken from the very top surface of the thin films with a sharp razor (Zeng et al., 2018). The spectra were recorded from 4000 cm⁻¹–400 cm⁻¹ using ATR-FTIR with an average of 32 scans at 4 cm⁻¹ resolution and background scans were subtracted before

each measurement. All spectra were analysed using the Essential FTIR v3.50.169 from Operant LLC. Manual baseline correction with a cubic spline was applied to all spectra in comparison. Multiple measurements were carried out for each sample for statistical analysis.

Differential scanning calorimetry (DSC)

Changes in the thermal properties (e.g. specific heat capacity c_p and glass transition temperature T_g) of all binders were evaluated using a TA Instruments Q250 Differential Scanning Calorimeter (DSC). For sample preparation, Tzero hermetic pans and hermetic lids were used to hold 10–20 mg of samples (including all asphalt binders and the rubber particles as obtained). To evaluate the UV aging effect, a thin film (< 1 mm) of material was taken from the very top surface of the UV aged samples with a sharp razor. No further drying process was applied to the samples before sealing the pan. The modulated DSC (MDSC) function was employed because it provides greater sensitivity than regular DSC, and it allows for differentiating between reversing and non-reversing thermal behaviours in materials (Masson et al., 2002). MDSC heating and cooling curves were obtained at different rates with a modulation period of 60 s and an amplitude of $\pm 0.47^\circ\text{C}$. A nitrogen cooling system was used for cooling and the nitrogen gas was purged at a rate of 50 ml/min. All samples were subjected to the following thermal cycles: (i) initial rapid cooling: after being equilibrated at 100°C , the samples were cooled to -60°C at a ramp rate of $10^\circ\text{C}/\text{min}$ and then held isothermal for 5 mins; (ii) first heating: -60°C to 100°C at $4^\circ\text{C}/\text{min}$ and then held isothermal for 5 mins; (iii) first cooling: 100°C to -60°C at $4^\circ\text{C}/\text{min}$ and then held isothermal for 5 mins; (iv) second heating: -60°C to 100°C at $4^\circ\text{C}/\text{min}$ and then held isothermal for 5 mins. Specific heat and glass transition temperature were determined from the second heating (i.e. step iv) as this cycle gives a more stable measurement of the sample's thermal property. At least three measurements were conducted for each sample for statistical analysis.

Flash method to measure thermal properties

In order to measure the thermal conductivity of the samples, the flash method was used. The flash method of measuring thermal diffusivity was first described by Parker in 1961 (Parker et al., 1961). Thermal diffusivity α (unit: mm^2/s) is a measure of the thermal inertia of a material. It gives an insight into how fast heat is propagated through the medium. Its concept is based on deriving thermal diffusivity from the thermal response of the rear side of an adiabatically insulated infinite plate whose front side is exposed to a short pulse of radiant energy. Several improvements to the model have been made. In 1963, Cowan took radiation and convection on the surface into account (Cowan, 1963). Cape and Lehman considered transient heat transfer, finite pulse effects and also heat losses in the same year (Cape & Lehman, 1963). Blumm and Opfermann improved the Cape-Lehman-Model with high order solutions of radial transient heat transfer and facial heat loss, non-linear regression routine in case of high heat losses and an advanced, patented pulse length correction (Blumm & Opfermann, 2002).

In this study, the Nanoflash LFA 447 from Netzsch Instruments was used to perform the measurements (Figure 3) according to the above flash method by following the ASTM E-1461 standard. The Nanoflash LFA 447 uses a high-performance Xenon flash lamp to produce the heat pulse on the front of the sample. The pulse width is adjustable between 0.06 and 0.3 ms. The measurement of the temperature increase on the rear of the sample is carried out with a liquid-nitrogen-cooled InSb (Indium-Antimonide) infrared detector. Both the detector and amplifier components are designed for measurements with a data acquisition rate of 500 kHz. The temperature in the sample holder is controlled by a furnace and can be set between room temperature and 300°C . A liquid sample holder with a diameter of 12.7 mm designed for low conductivity

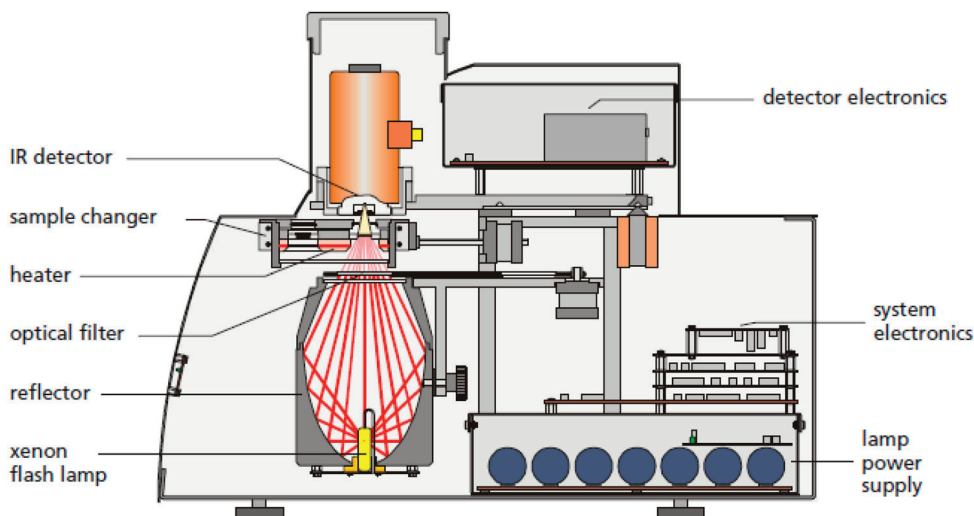


Figure 3. Overview of the Nanoflash LFA 447 apparatus.

materials was used for the measurements. The thickness of the samples was kept consistent in the range of 1–3 mm and was accurately measured. Three shots were applied to each sample and a suggested gain of 5012 at medium pulse width was used with a 20-second delay. All analyses were done using the Cowan model with pulse correction. The instrument was first calibrated with measuring the thermal conductivity of deionised water at 25°C and the results were within 1% deviation from the literature. Having determined the thermal diffusivity and the specific heat capacity, it is possible to derive the thermal conductivity of the samples:

$$\lambda = \alpha \cdot c_p \cdot \rho \quad (2)$$

where α is the thermal diffusivity, c_p is the specific heat and ρ is the bulk density.

Dynamic shear rheometer (DSR)

To evaluate changes in the rheological properties of the neat binder and rubber-modified binders before and after UV aging at medium to high temperatures, a Bohlin Gemini II dynamic shear rheometer (DSR) from Malvern Instruments was used. This instrument can be operated within the range of room temperature to 300°C, although to run samples at temperatures below 25°C, it needs to be connected to a liquid nitrogen inlet. In this study, an oscillation mode was conducted in accordance with AASHTO T315-10, running a frequency sweep test from 0.1 to 100 rad/s with 1% controlled strain in the temperature range of 34°C to 88°C with an increment of 6°C and an accepted tolerance of $\pm 0.1^\circ\text{C}$. A temperature calibration of 300 s and an integration time of 200 s with 5 s delay were chosen to make sure the sample has been equilibrated and reached a steady temperature before running the oscillation at each temperature. The ETCPP25 parallel geometry plates (25 mm in diameter) were used to perform all tests. The gap size was set to 1 mm and a 7% trimming gap was considered (1.070 mm) to produce a bulge after the sample has been trimmed. This is necessary to make sure after trimming, a disk shape geometry is formed to achieve accurate measurements. Master curves were generated using the time-temperature superposition (TTS) principle with a reference temperature of 58°C. From the output file, measured parameters such as complex modulus, complex viscosity, and phase angle were used to analyse the results.

Scanning electron microscope (SEM)

A Philips FEI (XL20) SEM was used to study the microscopic morphologies of the asphalt binders. Image formation in an electron microscope requires a high vacuum environment. Thus, the drying of samples was a prerequisite for viewing and obtaining good images in normal high vacuum SEM system. A rotary and a diffusion pump were used to vacuum-seal the samples at a maximum vacuum level of 1×10^{-4} torr. The metallisation process was performed using the aluminium coating. Coating of samples is required to make the samples conductive to avoid charging of electrons as well as to reduce thermal damage and improve the secondary electron signal required for topographic examination in the SEM. Therefore, a thin layer of aluminium (with a thickness of about 8 ± 3 Å) was coated on all samples. It should be noted that the increase in temperature during the coating phase is negligible with respect to the heating generated by the electron beam during SEM scanning.

Results and discussion

FTIR results

FTIR spectra of all six samples are shown in Figure 4 and it seems that the UV aging is the dominant factor causing differences in the spectra. No obvious difference was seen in the IR spectra of the three unaged samples (neat, 16.6% and 20.0% rubber binders), indicating that adding rubber particles did not cause any significant difference in the rubber-modified binders compared with the neat binder.

After 100 h of UV aging, a few distinct changes occurred in the IR spectra. For instance, the aromatic stretching vibrations at 1600 cm^{-1} evolved to be two split peaks at 1577 and 1540 cm^{-1} . Carboxylic acid C = O stretching (1710 cm^{-1}) appeared in all three UV aged samples. In addition, a broad strong peak in the range of $3200\text{--}3550 \text{ cm}^{-1}$ is identified in the three UV aged samples, which is attributed to alcohol/phenol O-H stretching (Lins et al., 2008). These changes

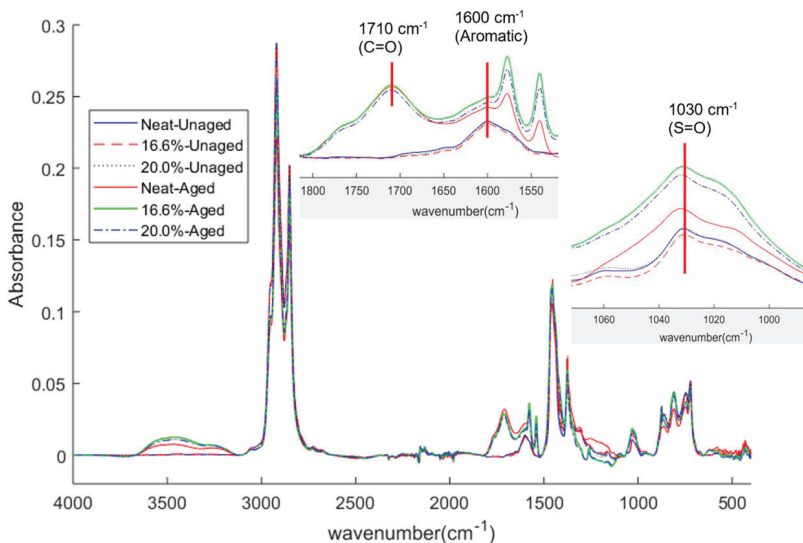


Figure 4. ATR-FTIR spectra of unaged and UV aged neat binder, 16.6% CR-modified binder, and 20.0% CR-modified binder. The insets show zoomed-in absorbance peaks at 1710 cm^{-1} (C = O), 1600 cm^{-1} (aromatic groups), and 1030 cm^{-1} (S = O).

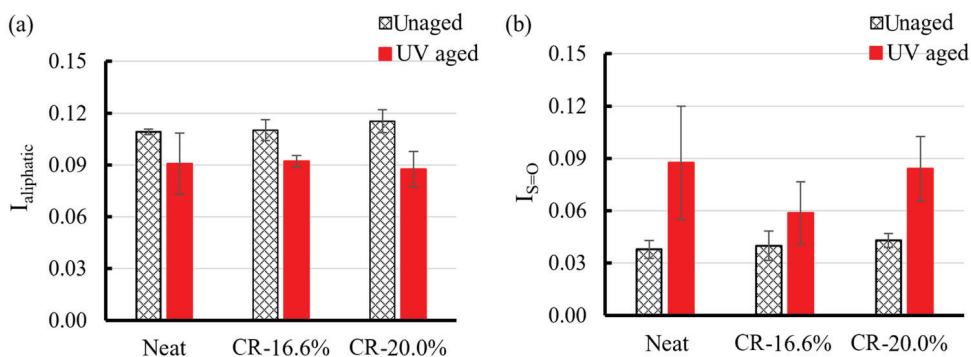


Figure 5. (a) Aliphatic index, and (b) sulphoxide index of unaged and UV aged neat binder, 16.6% and 20.0% crumb rubber (CR)-modified binders.

in the IR spectra due to UV aging have also been reported in other literature (de Sá et al., 2013; Feng et al., 2013; Mouillet et al., 2008).

For quantitative analysis, structural indices of the aliphatic bond (1376 cm^{-1}) and sulphoxide bond (1030 cm^{-1}) were calculated to compare their intensity differences due to the addition of CR particles and UV aging. This is done by normalising the area under these peaks by the total area of the spectral bands between $600\text{--}2000\text{ cm}^{-1}$ (Feng et al., 2013; Mouillet et al., 2008). The aliphatic ($I_{\text{aliphatic}}$) and sulphoxide ($I_{S=O}$) indices are shown in Figure 5(a,b), respectively. Standard deviations for the two indices are smaller for the three unaged samples than those for the UV-aged samples. Such a difference is probably due to the challenge in controlling the depth when scraping the thin layer of material off the surface of the UV-aged samples. The neat-unaged, 16.6%-unaged, and 20.0%-unaged had comparable aliphatic and sulphoxide indices, consistent with the earlier qualitative comparison. The three UV aged samples had smaller aliphatic indices and larger sulphoxide indices, indicating that the samples went through oxidation during UV aging. This is in agreement with other researchers (Feng et al., 2013; Lins et al., 2008; Mouillet et al., 2008). Among all three UV-aged samples, the 16.6%-aged had the smallest sulphoxide index (by average values). Therefore, it is likely that the 16.6% rubber binder could have better UV aging resistance than the 20.0% rubber binder in terms of oxidation prevention.

DSC results

Specific heat of all six samples increased slowly as a function of temperature, with a rate of $(0.0029\text{--}0.0035)\text{ J/g}\cdot^{\circ}\text{C}$ per Celsius degree in a temperature range 25°C to 40°C (data not shown). Figure 6(a) shows the specific heat of all six samples at 30°C . For unaged samples, adding rubber particles into neat binder PG 64–22 produced rubberised binders with slightly lower specific heat values on average. This may be caused by mixing of rubber with the binder where rubber particles with lower specific heat (i.e. 15% less than that of the unaged neat binder) reduced the specific heat of the CR-modified binders. Reduction in specific heat capacity for CR-modified binders relative to the neat binder found in this study is consistent with findings from Chen et al. (2015) in which recycled tire rubber was used to improve the heat insulation performance of asphalt binders and mixtures. However, the specific heat of unaged 16.6% and unaged 20.0% CR-modified binders did not appear to decrease proportionally with respect to the unaged neat binder (i.e. 0% of CR) and the reason for this should be investigated in our future work.

After 100 h of UV aging, interestingly, the specific heat of all three samples increased but to different extents. Specific heat of UV aged 16.6% increased the most (i.e. by 29% as compared

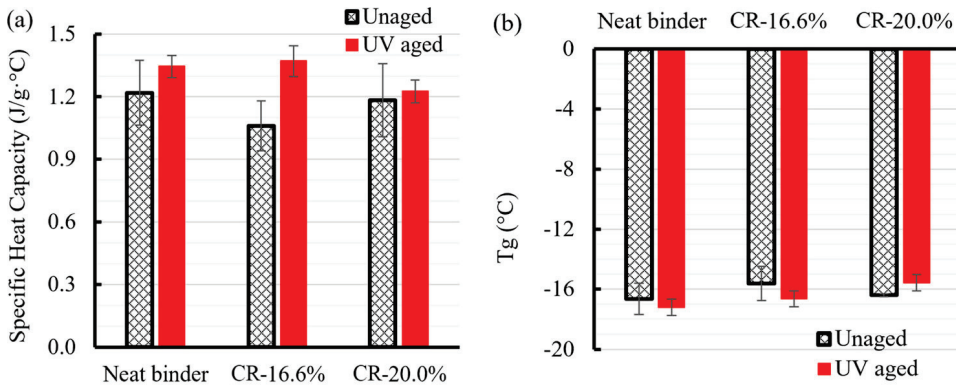


Figure 6. (a) Specific heat capacity, and (b) glass transition temperature of neat binder, 16.6% and 20.0% crumb rubber (CR)-modified binders without and with 100-hour UV aging.

to its unaged counterpart), and it is also 2% higher than that of the neat binder on average. The UV aged 20.0% had the lowest specific heat, 24% smaller than that of the neat binder on average. It seems that adding 16.6% CR produced binder with better UV aging resistance as compared to the neat and the 20.0% CR in terms of specific heat change. However, to answer what weight percentage of CR produces rubber-modified binders with overall better thermal properties after UV aging, further evaluation of the thermal conductivity of these samples is required.

Figure 6(b) and Figure 7 show that all samples had a strong glass transition centred around -16°C , regardless of the sample type or aging conditions. The two rubberised binders (16.6% and 20.0%) had glass transitions at slightly higher temperatures (i.e. the absolute values of T_g is smaller) than that of the neat binder, and this is independent of the aging condition. The higher T_g s in CR-modified binders can be attributed to the stiffening effect of the rubber particles (Lo Presti, 2013). However, adding CR particles into this specific type of neat binder did not likely cause any phase instability issue in the CR-modified binders because the derivatives curves in Figure 8 for samples in both the unaged and UV aged groups follow similar trends. UV aging led to more pronounced secondary weak T_g s within -5°C to 25°C , indicating that chemical incompatibility or phase separation might have occurred in the UV aged samples.

Nanoflash results

Figure 8 shows the thermal conductivity values of all samples measured from the Nanoflash. It can be seen that for both unaged and UV aged samples, the thermal conductivity increases as the temperature increases. However, as compared to the two rubber-modified binders, the neat binder has a larger increasing rate in its thermal conductivity as a function of temperature. Thermal conductivity decreases with an increase in the rubber powder content, with the unaged 20.0% sample having the lowest thermal conductivity. Such a trend can be attributed to the lower conductivity value of the crumb rubber as compared to the neat binder; the same mixture effect as mentioned in the specific heat values measured by the DSC. From the paving practice point of view, the larger the thermal conductivity, the faster the trapped heat in the pavement can be dissipated, thus resulting in less overall thermal cracking. However, the relaxation capability of the pavement should also be considered, since a faster heat propagation in the pavement with low relaxation capability could cause thermal stress and eventually cracking in the pavement.

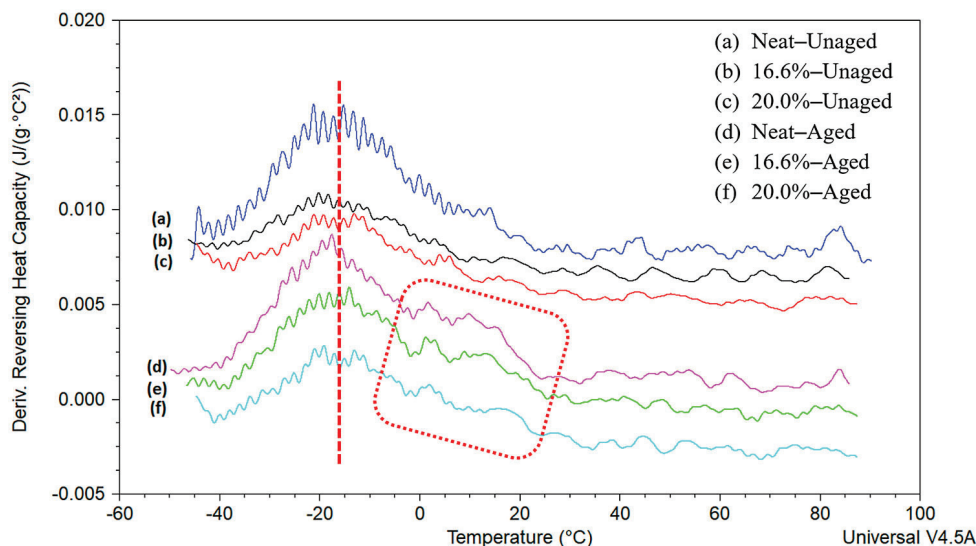


Figure 7. The derivative of reversing heat capacity with respect to temperature for unaged and UV-aged neat binder, 16.6% and 20.0% CR-modified binders. All six samples showed a strong T_g around -16°C (highlighted in the vertical red dotted line). As compared to the unaged samples, the UV aged samples displayed secondary T_g s within -5°C to 25°C (highlighted in the red rounded rectangle).

Reduction in thermal conductivity of CR-modified binders could lead to some early age thermal-related distress within asphalt binders. The UV aging effect on thermal conductivity of asphalt concrete using CR-modified binders can provide more insights into distresses in the pavement.

After UV aging, the thermal conductivity decreases for pure and rubber-modified samples, as compared to the corresponding unaged samples. This is true for all three temperatures that were measured (i.e. 30°C , 35°C , and 40°C). The neat binder and the 16.6% rubber binder have higher drops after UV aging whereas the 20.0% rubber binder only has a slight reduction after UV aging. To make a more comprehensive evaluation of the thermal properties of the neat binder as well as the CR-modified binders before and after UV aging, the trend in the thermal conductivity (measured from Nanoflash) of the six samples was compared with that of their corresponding specific heat (measured from DSC). It was found that differences in the thermal conductivity among these samples are more significant than those in their specific heat. Therefore, thermal conductivity might be the dominant factor to evaluate the effect of UV aging on binders' thermal properties. In that sense, before UV aging, 16.6% rubber binder has the best thermal performance whereas, after UV aging, 20.0% rubber binder would have a slightly better thermal performance. This is consistent with the anti-oxidation effect of UV absorber modified binder (Feng et al., 2013; Mouillet et al., 2008; Ruan et al., 2003).

DSR results

In Figure 9(a–c), the complex moduli of samples as a function of reduced angular frequency are shown on a log–log basis. It can be seen that the CR-modified binders have a higher complex modulus at medium and low frequencies (high temperatures), thus, are stiffer than the neat binder. The binder modified with a higher rubber percentage has a higher complex modulus than the one with a lower rubber percentage and this is true for both unaged and UV aged samples. However, the effect of rubber percentage on complex modulus seems to be smaller in the UV aged samples. It can be concluded that exposing the samples to UV rays has caused an increase

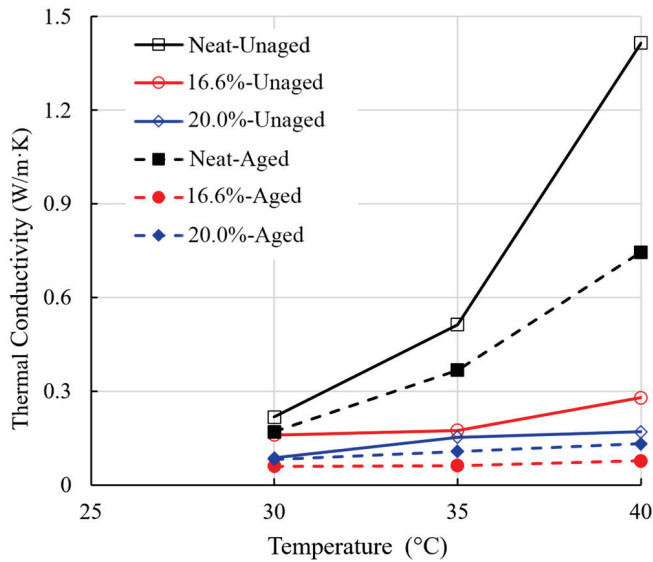


Figure 8. Thermal conductivity results for unaged and UV aged neat binder, 16.6% and 20.0% CR-modified binders at 30°C, 35°C, and 40°C.

in their complex modulus. For the neat binder, aging caused a 42.3% increase in the complex modulus values (on average of all the frequencies of the master curve), whereas, for 16.6% rubber binder, this change is only 18.2% increase. For 20.0% CR-modified binder, UV aging causes a 19.0% increase on average for G^* compared to the unaged samples. Overall, the complex modulus of 16.6% CR-modified binder was less affected by the ultraviolet exposure, especially at mid and higher frequencies (low temperatures) compared to both the neat and 20.0% rubber samples. Moreover, the phase angle as a function of reduced angular frequency curve for the two CR-modified binders seems to have a bell-shape whereas for neat binder the curve is more of a typical curve. The authors speculate that this observation is due to the addition of the rubber particles which has formed a network after swelling inside the asphalt binder and thus, a pseudo-solid behaviour is observed. The aforementioned findings could also be the results of the addition of elastic components (rubber) to the binder, which begin to act as particulate solid when the base asphalt presents liquid behaviours. To further verify this inference, the complex viscosity versus complex modulus of all six samples were plotted and the trends were examined.

The complex viscosity versus the shear complex modulus curves for all samples is shown in Figure 10. While the measurements for both unaged and aged neat samples show a Newtonian behaviour representing a typical liquid response (Qin et al., 2014b), it is obvious that with the addition of the rubber, the viscosity diverges and a more sol-gel or pseudo-solid behaviour is observed. This observation can be attributed to the microstructure changes of asphalt binder when rubber particles are added, and formation of networks or semi-solid structures which alter the temperature dependence of the samples. These findings are in-line with the complex modulus and phase angle outputs from the previous part.

Figure 11 compares the rutting and fatigue parameters before and after UV aging for different percentages of rubber particles. Pavement design requires that asphalt concrete should be stiff enough to resist rutting especially during the early and mid-life of the pavement. With every traffic cycle on the road, loading and unloading happen on the pavement. Part of the work is recovered from the elastic portion of the binder, whereas the other parts are dissipated in the pavement as heating, cracking, and permanent deformation (Guide, 2002). The work being

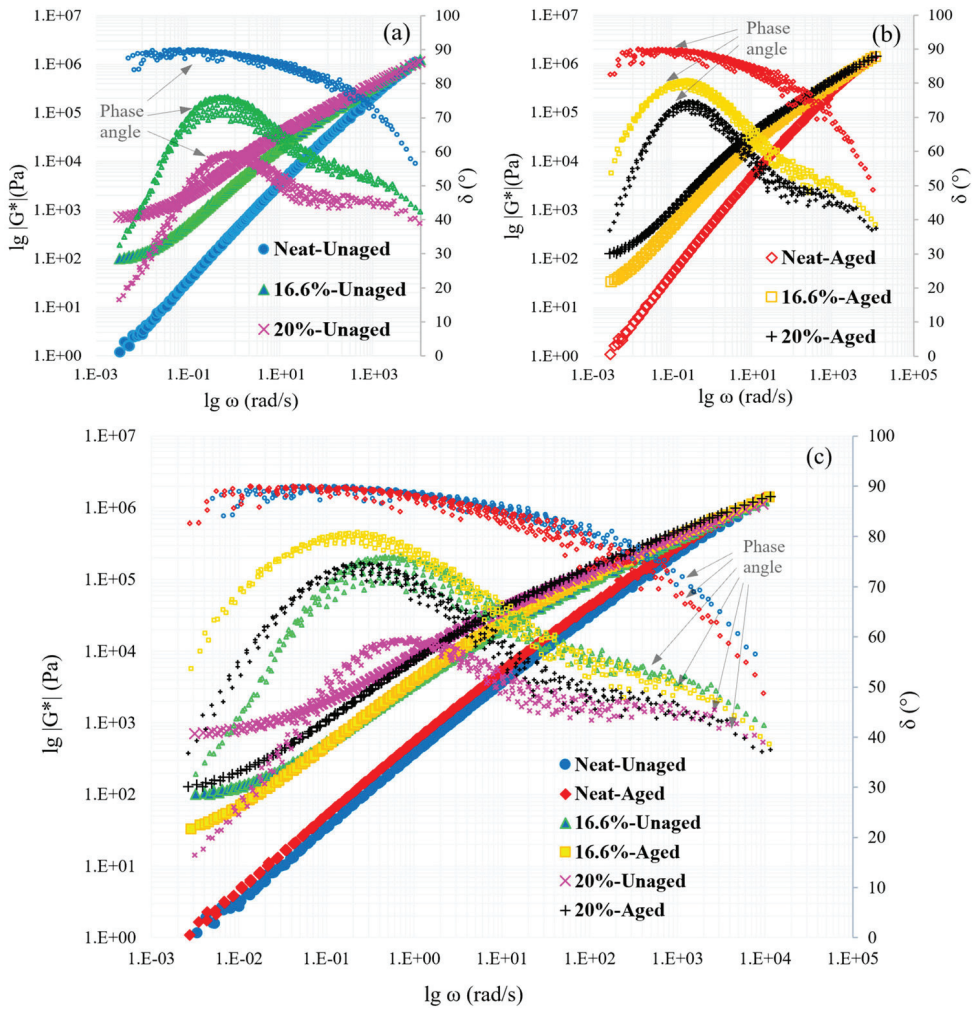


Figure 9. Complex shear modulus and phase angle versus angular frequency of (a) unaged samples, (b) aged samples, and (c) both unaged and aged samples.

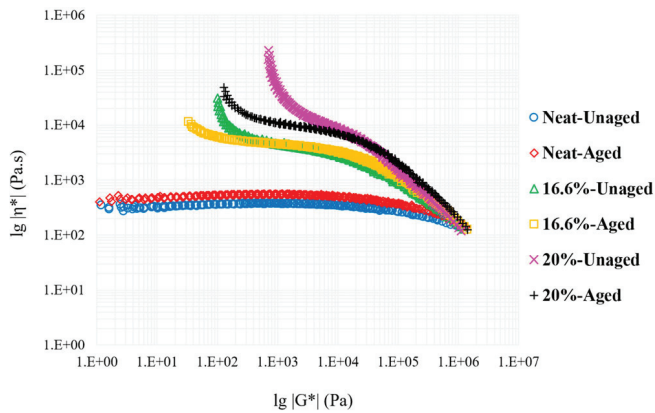


Figure 10. Complex viscosity as a function of complex modulus.

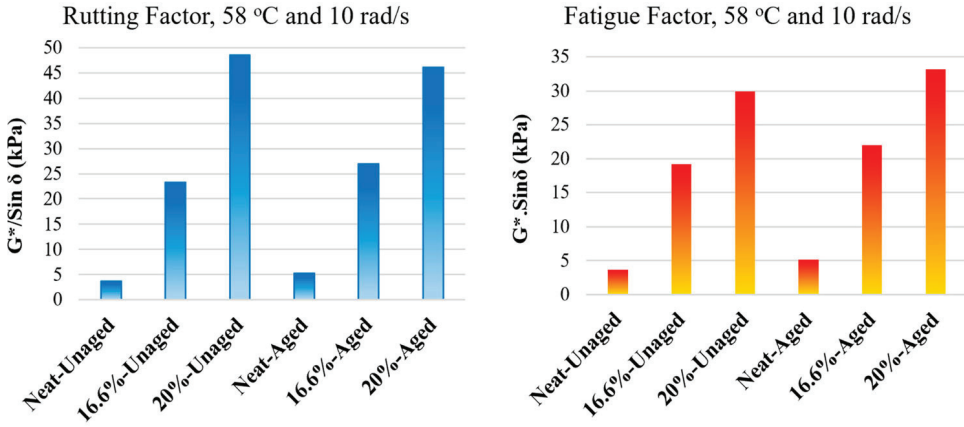


Figure 11. Calculated rutting factor and fatigue factor of the samples.

dissipated at constant stress at every cycle can be expressed as:

$$W_c = \pi \sigma_o^2 \left[\frac{1}{G^*/\sin\delta} \right] \quad (3)$$

In which W_c is the work dissipated per load cycle, σ_o is the applied stress, G^* is the complex modulus, and δ is the phase angle. Therefore, in order to minimise the W_c , the $G^*/\sin\delta$ should be maximised. It is observed that adding rubber particles to the asphalt binder increases the rutting parameter. While for neat and 16.6% rubber samples, UV aging causes an increase in the rutting parameter, for 20.0% rubber sample, this factor decreases by 5.3%. It seems that for the experiment, the 16.6% rubber asphalt showed the best rutting performance when subjected to UV aging.

In addition to rutting resistance, an asphalt pavement should be elastic enough to resist fatigue cracking. The work that is dissipated at a constant strain per each cycle is defined as:

$$W_c = \pi \epsilon_o^2 [G^* \sin\delta] \quad (4)$$

In which, W_c is the work dissipated per load cycle, ϵ_o is the strain during the load cycle, G^* is the complex modulus, and δ is the phase angle. Here, the lower values of the term $G^* \cdot \sin\delta$ will result in less fatigue cracking. Figure 11 shows that the neat binder has the lowest fatigue parameter for both unaged and UV aged samples. Addition of rubber to the binder affects its fatigue performance in an adverse way significantly. However, for rubber-modified samples, the 16.6% sample has a lower $G^* \sin\delta$ compared to the 20.0% rubber sample. Overall, considering both rutting and fatigue factors, it can be concluded that the 16.6% CR-modified binder has the best performance to satisfy both parameters.

SEM results

A Scanning Electron Microscope (SEM) with a magnification of 25 ~ 500X was used to understand more thoroughly the influence of UV aging on the microscopic morphology of the neat and CR-modified binders. The unaged binder (Figure 12) appears to have a single-phase continuous yet non-uniform structure, and the presence of crumb rubber was not clearly traceable in the images. After going under UV exposure, interlaced cracks were observed on the surface of the aged samples (Figure 13). The orthogonal pattern of the cracks in UV aged samples leads

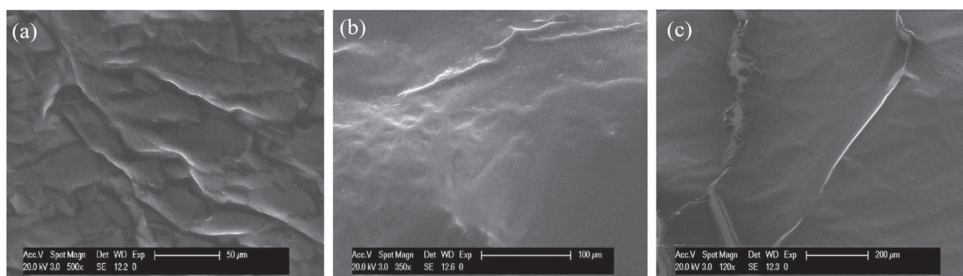


Figure 12. Morphology of (a) neat binder, (b) 16.6% CR-modified binder, and (c) 20.0% CR-modified binder before UV aging.

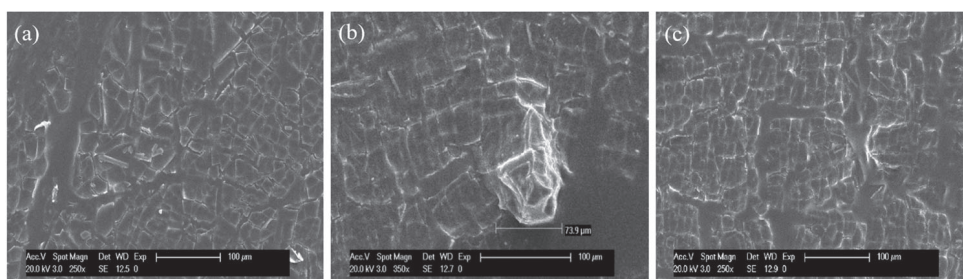


Figure 13. Morphology of (a) neat binder, (b) 16.6% CR-modified binder, and (c) 20.0% CR-modified binder after UV aging.

to the formation of rectangular and isolated polygons and it seems that as the rubber percentage increases the size of the cracks decrease while the cracks form a more organised square shape network. With the presence of rubber in asphalt, the cracked binder seems to still hold itself together whereas, in the neat binder, a more brittle structure is observed.

Conclusions

This research aimed to investigate the effect of simulated ultraviolet (UV) radiation from the sunshine on the asphalt binder containing recycled crumb rubber. To do so, three samples with 0, 16.6, and 20 wt. % of crumb rubber were prepared, and their chemical, thermal, rheological, and microscopic morphological properties before and after the UV exposure were characterised and compared. The following findings were achieved:

- (1) Addition of rubber did not cause any obvious change in FTIR spectra from both qualitative comparison and the numerical aliphatic index and sulphoxide index. UV aging caused oxidation for all three samples, as evidenced by the reduced aliphatic index and increased sulphoxide index.
- (2) The unaged rubber-modified binders had a lower specific heat due to the small specific heat of the CR particles that replaced the corresponding proportion of neat binder. UV aging resulted in higher specific heat values for all three samples, with the 16.6%-aged having the highest specific heat. Addition of rubber made the glass transition shift to a slightly higher temperature, which is attributed to the stiffening effect of the rubber particles to asphalt binder. Yet, no chemical incompatibility was observed when adding the CR particles to this specific type of neat binder, which agrees with the FTIR results. All three UV aged samples showed possible secondary glass transitions, indicating

that chemical incompatibility or phase separation might have occurred when subjected to UV aging.

- (3) Among the three UV aged samples, the UV aged 16.6% CR-modified binder had the smallest sulphoxide index and the highest specific heat.
- (4) Thermal conductivity might be the dominant factor to evaluate the effect of UV aging on the thermal properties of samples, whereas specific heat is the secondary factor. Thus, 16.6% rubber binder had a better thermal performance before UV aging whereas 20.0% rubber binder had a slightly better thermal performance when subjected to UV aging.
- (5) Complex moduli of the samples increased after UV aging and this increase was the most for the neat binder and the least for 16.6% CR-modified binder.
- (6) Rutting parameter increased with UV aging in both the neat and the 16.6% rubber samples; however, it decreased by 5.3% after UV aging for 20% rubber-modified sample.
- (7) Fatigue factor increased by the addition of rubber particles and also after UV aging for all the specimens. For 16.6% rubber binder, this increase was less which is more favourable.
- (8) A semi-solid behaviour is observed when the CR particles are added to the asphalt binder. This observation is believed to be related to the swelling and formation of a micro-network among the rubber particles.
- (9) Morphological analysis showed that when crumb rubber modified asphalt is exposed to UV aging, cracks are formed in microscale, and the size of the cracks are smaller with higher percentage of rubber, and the presence of rubber seemed to hold the cracked asphalt together, whereas in the neat asphalt after UV aging, the cracked asphalt pieces seemed to be separated from each other.

Research significance

The novelty of this work was to address a type of photo-oxidation – the ultraviolet aging from sunlight – on a mix of asphalt and rubber, which is becoming a more common practice in the asphalt industry as a solution for promoting sustainability and recycling. The new rubber-modified roads, while providing many benefits such as noise reduction of tires, less oxidation, and accordingly longer service life, are more complicated and thus different aspects of them need to be studied. The performance of the pavement under sunlight and the UV rays is one of those aspects that affect the long term behaviour of the asphalt. Future works can include other tests on the mixture of aggregates and rubber modified binder to see how an actual mixture with rubber behaves under the photo-oxidation of sunlight.

Acknowledgements

This study has been sponsored by the NSF IIP 1738802 and CMMI 1762891, whose supports are gratefully acknowledged. The authors would like to thank the Carleton Lab managers (Dr. Liming Li, Dr. Adrian Brugger, and Mr. William B. Blanke) and Dr. Fangliang Chen from Schuco USA LLLP for their support and help in this project. Also, the authors show their appreciation to Peckham Industries Inc. and Mr. Bob Yaremko for graciously providing the asphalt binder. The authors are also thankful to Dr. Karen M. Wovkulich at Vassar College for letting us use the FTIR, Dr. Sanat K. Kumar from Columbia University for allowing us to use the DSC, and Professor Andrea Saccani at DICAM, University of Bologna, for his help with performing the SEM analysis. The contents of this paper reflect the view of the authors, who are responsible for the facts and the accuracy of the data presented. This paper does not constitute a standard, specification, or regulation.

References

- Abdelrahman, M., & Carpenter, S. (1999). Mechanism of interaction of asphalt cement with crumb rubber modifier. *Transportation Research Record: Journal of the Transportation Research Board*, 1661, 106–113. <https://doi.org/10.3141/1661-15>

- Bahia, H., Zhai, H., & Rangel, A. (1998). Evaluation of stability, nature of modifier, and short-term aging of modified binders using new tests: LAST, PAT, and modified RTFO. *Transportation Research Record: Journal of the Transportation Research Board*, 1638, 64–71. <https://doi.org/10.3141/1638-08>
- Blumm, J., & Opfermann, J. (2002). Improvement of the mathematical modeling of flash measurements. *High Temperatures-High Pressures*, 34(5), 515–521. <https://doi.org/10.1068/hjtr061>
- Cape, J., & Lehman, G. W. (1963). Temperature and finite pulse-time effects in the flash method for measuring thermal diffusivity. *Journal of Applied Physics*, 34(7), 1909–1913. <https://doi.org/10.1063/1.1729711>
- Chen, M., Zheng, J., Li, F., Wu, S., Lin, J., & Wan, L. (2015). Thermal performances of asphalt mixtures using recycled tire rubber as a mineral filler. *Road Materials and Pavement Design*, 16(2), 379–391. <https://doi.org/10.1080/14680629.2014.1002524>
- Cortizo, M. S., Larsen, D. O., Bianchetto, H., & Alessandrini, J. L. (2004). Effect of the thermal degradation of SBS copolymers during the aging of modified asphalts. *Polymer Degradation and Stability*, 86(2), 275–282. <https://doi.org/10.1016/j.polymdegradstab.2004.05.006>
- Cowan, R. D. (1963). Pulse method of measuring thermal diffusivity at high temperatures. *Journal of Applied Physics*, 34(4), 926–927. <https://doi.org/10.1063/1.1729564>
- de Sá, M. D. F. A., Lins, V. D. F. C., Pasa, V. M. D., & Leite, L. F. M. (2013). Weathering aging of modified asphalt binders. *Fuel Processing Technology*, 115, 19–25. <https://doi.org/10.1016/j.fuproc.2013.03.029>
- Feng, Z. G., Yu, J. Y., Zhang, H. L., Kuang, D. L., & Xue, L. H. (2013). Effect of ultraviolet aging on rheology, chemistry and morphology of ultraviolet absorber modified bitumen. *Materials and Structures*, 46(7), 1123–1132. <https://doi.org/10.1617/s11527-012-9958-3>
- Guide, R. D. (2002). *Roadside design guide, 4th edition, includes errata (2015)*. American Association of State Highway and Transportation Officials.
- Huang, S. C., & Pauli, A. T. (2008). Particle size effect of crumb rubber on rheology and morphology of asphalt binders with long-term aging. *Road Materials and Pavement Design*, 9(1), 73–95. <https://doi.org/10.1080/14680629.2008.9690108>
- Lewandowski, L. H. (1994). Polymer modification of paving asphalt binders. *Rubber Chemistry and Technology*, 67(3), 447–480. <https://doi.org/10.5254/1.3538685>
- Lins, V. F. C., Araújo, M. F. A. S., Yoshida, M. I., Ferraz, V. P., Andrada, D. M., & Lameiras, F. S. (2008). Photodegradation of hot-mix asphalt. *Fuel*, 87(15–16), 3254–3261. <https://doi.org/10.1016/j.fuel.2008.04.039>
- Lo Presti, D. (2013). Recycled tire rubber modified bitumens for road asphalt mixtures: A literature review. *Construction and Building Materials*, 49, 863–881. <https://doi.org/10.1016/j.conbuildmat.2013.09.007>
- Lu, X., & Isacson, U. (1998). Chemical and rheological evaluation of aging properties of SBS polymer modified bitumens. *Fuel*, 77(9–10), 961–972. [https://doi.org/10.1016/S0016-2361\(97\)00283-4](https://doi.org/10.1016/S0016-2361(97)00283-4)
- Lu, X., & Isacson, U. (2002). Effect of aging on bitumen chemistry and rheology. *Construction and Building Materials*, 16(1), 15–22. [https://doi.org/10.1016/S0950-0618\(01\)00033-2](https://doi.org/10.1016/S0950-0618(01)00033-2)
- Masson, J. F., Polomark, G. M., & Collins, P. (2002). Time-dependent microstructure of bitumen and its fractions by modulated differential scanning calorimetry. *Energy & Fuels*, 16(2), 470–476. <https://doi.org/10.1021/ef010233r>
- Medina, J. R., & Underwood, B. S. (2017). Micromechanical shear modulus modeling of activated crumb rubber modified asphalt cements. *Construction and Building Materials*, 150, 56–65. <https://doi.org/10.1016/j.conbuildmat.2017.05.208>
- Mouillet, V., Farcas, F., & Besson, S. (2008). Aging by UV radiation of an elastomer modified bitumen. *Fuel*, 87(12), 2408–2419. <https://doi.org/10.1016/j.fuel.2008.02.008>
- Mrawira, D. M., & Luca, J. (2002). Thermal properties and transient temperature response of full-depth asphalt pavements. *Transportation Research Record*, 1809(1), 160–171. <https://doi.org/10.3141/1809-18>
- Ouyang, C., Wang, S., Zhang, Y., & Zhang, Y. (2006). Improving the aging resistance of styrene–butadiene–styrene tri-block copolymer modified asphalt by addition of antioxidants. *Polymer Degradation and Stability*, 91(4), 795–804. <https://doi.org/10.1016/j.polymdegradstab.2005.06.009>
- Parker, W. J., Jenkins, R. J., Butler, C. P., & Abbott, G. L. (1961). Flash method of determining thermal diffusivity, heat capacity, and thermal conductivity. *Journal of Applied Physics*, 32(9), 1679–1684. <https://doi.org/10.1063/1.1728417>
- Pietrak, K., & Wisniewski, T. S. (2014). A review of models for effective thermal conductivity of composite materials. *Journal of Power Technologies*, 95(1), 14–24. <http://papers.itc.pw.edu.pl/index.php/JPT/article/view/463/637>

- Qin, Q., Farrar, M. J., Pauli, A. T., & Adams, J. J. (2014b). Morphology, thermal analysis and rheology of Sasobit modified warm mix asphalt binders. *Fuel*, *115*, 416–425. <https://doi.org/10.1016/j.fuel.2013.07.033>
- Qin, Q., Schabron, J. F., Boysen, R. B., & Farrar, M. J. (2014a). Field aging effect on chemistry and rheology of asphalt binders and rheological predictions for field aging. *Fuel*, *121*, 86–94. <https://doi.org/10.1016/j.fuel.2013.12.040>
- Ruan, Y., Davison, R. R., & Glover, C. J. (2003). The effect of long-term oxidation on the rheological properties of polymer modified asphalts*. *Fuel*, *82*(14), 1763–1773. [https://doi.org/10.1016/S0016-2361\(03\)00144-3](https://doi.org/10.1016/S0016-2361(03)00144-3)
- Tarefder, R. A., Zaman, M., & Hobson, K. (2003). A laboratory and statistical evaluation of factors affecting rutting. *International Journal of Pavement Engineering*, *4*(1), 59–68. <https://doi.org/10.1080/10298430310001593263>
- Wu, S., Han, J., Pang, L., Yu, M., & Wang, T. (2012). Rheological properties for aged bitumen containing ultraviolet light resistant materials. *Construction and Building Materials*, *33*, 133–138. <https://doi.org/10.1016/j.conbuildmat.2012.01.019>
- Yi-Qiu, T., Jia-Ni, W., Xing-Ye, Z., & Hui-Ning, X. U. (2008). Ultraviolet aging mechanism of asphalt binder. *China Journal of Highway and Transport*, *1*, 89. <http://zgglxb.chd.edu.cn/EN/abstract/abstract632.shtml>
- Yildirim, Y. (2007). Polymer modified asphalt binders. *Construction and Building Materials*, *21*(1), 66–72. <https://doi.org/10.1016/j.conbuildmat.2005.07.007>
- Yu, X., Zaumanis, M., Dos Santos, S., & Poulidakos, L. D. (2014). Rheological, microscopic, and chemical characterization of the rejuvenating effect on asphalt binders. *Fuel*, *135*, 162–171. <https://doi.org/10.1016/j.fuel.2014.06.038>
- Zadshir, M., Hosseinezhad, S., Ortega, R., Chen, F., Hochstein, D., Xie, J., & Fini, E. H. (2018). Application of a biomodifier as Fog Sealants to delay ultraviolet aging of Bituminous materials. *Journal of Materials in Civil Engineering*, *30*(12), 04018310. [https://doi.org/10.1061/\(ASCE\)MT.1943-5533.0002483](https://doi.org/10.1061/(ASCE)MT.1943-5533.0002483)
- Zeng, W., Wu, S., Pang, L., Chen, H., Hu, J., Sun, Y., & Chen, Z. (2018). Research on Ultra Violet (UV) aging depth of asphalts. *Construction and Building Materials*, *160*, 620–627. <https://doi.org/10.1016/j.conbuildmat.2017.11.047>
- Zeng, W., Wu, S., Wen, J., & Chen, Z. (2015). The temperature effects in aging index of asphalt during UV aging process. *Construction and Building Materials*, *93*, 1125–1131. <https://doi.org/10.1016/j.conbuildmat.2015.05.022>